ISSN 1027-5495. Functional Materials, 28, No.1 (2021), p. 6-13.
doi:https://doi.org/10.15407/fm28.01.6

Temperature quenching of Ce^{3+} emission in gadolinium-aluminum garnet $Gd_3Al_5O_{12}$

***I.V.Berezovskaya*[1], *A.S.Voloshinovskii*[2], *Z.A.Khapko*[2], *O.V.Khomenko*[1], *N.P.Efryushina*[1], *V.P.Dotsenko*[1]**

[1]A.Bogatsky Physico-Chemical Institute, National Academy of Sciences of Ukraine, 86 Lustdorfskaya doroga, 65080 Odesa, Ukraine
[2]I.Franko National University of Lviv, 8 Kyryla i Mefodiya Str., 79005 Lviv, Ukraine

Received August 28, 2020

Gadolinium aluminum garnet (GAG) doped with Ce^{3+} ions was prepared by a co-precipitation method. The luminescent properties of Ce^{3+} ions in $Gd_{3(1-x)}Ce_{3x}Al_5O_{12}$ (x = 0.01) were studied in the temperature range of 77–500 K. At 77 K, the Ce^{3+} doped GAG exhibits broad-band emission with a maximum at 564 nm and a decay time of 68.4 ns. It was shown that the temperature quenching of the Ce^{3+} emission in GAG starts at 310 K and the quenching temperature ($T_{50\%}$) is 395 K. From the temperature dependence of the luminescence decay time upon excitation in the region of the Ce^{3+} $4f\rightarrow5d_{1,2}$ absorption bands, the activation energy for the Ce^{3+} emission quenching in GAG was found to be 0.51 eV. The quenching mechanism in Ce^{3+}-doped GAG was determined as the thermally induced ionization of Ce^{3+} ions.

Keywords: oxides, chemical synthesis, luminescence, cerium, quenching.

Температурне гасіння люмінесценції Ce^{3+} у гадоліній алюмінієвому гранаті $Gd_3Al_5O_{12}$. *І.В.Березовська, А.С.Волошиновський, З.А.Хапко, О.В.Хоменко, Н.П.Єфрюшина, В.П.Доценко.*

Гадоліній алюмінієвий гранат (GAG), легований іонами Ce^{3+}, отримано методом співосадження. Люмінесцентні властивості іонів Ce^{3+} у $Gd_{3(1-x)}Ce_{3x}Al_5O_{12}$ (x = 0,01) досліджено в інтервалі температур 77–500 К. При 77 К легований Ce^{3+} GAG демонструє широкосмугове випромінювання з максимумом при 564 нм і часом загасання люмінесценції 68,4 нс. Встановлено, що температурне гасіння люмінесценції Ce^{3+} у GAG починається при 310 К, а температура гасіння ($T_{50\%}$) становить 395 К. З температурної залежності часу загасання люмінесценції при збудженні в області смуг поглинання $4f\rightarrow5d_{1,2}$ іонів Ce^{3+} знайдено, що енергія активації гасіння люмінесценції Ce^{3+} у GAG становить 0,51 еВ. Механізм температурного гасіння люмінесценції Ce^{3+} GAG визначено як термічно індукована іонізація іонів Ce^{3+}.

Гадолиний алюминиевый гранат (GAG), легированный ионами Ce^{3+}, получен методом соосаждения. Люминесцентные свойства ионов Ce^{3+} в $Gd_{3(1-x)}Ce_{3x}Al_5O_{12}$ (x = 0,01) исследованы в интервале температур 77–500 К. При 77 К легированный Ce^{3+} GAG демонстрирует широкополосное излучение с максимумом при 564 нм и временем затухания люминесценции 68,4 нс. Установлено, что температурное тушение люминесценции Ce^{3+} в GAG начинается при 310 К, а температура тушения ($T_{50\%}$) составляет 395 К. Из температурной зависимости времени затухания люминесценции при возбуждении в области полос поглощения $4f\rightarrow5d_{1,2}$ ионов Ce^{3+} найдено, что энергия активации тушения люминесценции Ce^{3+} в GAG составляет 0,51 эВ. Механизм температурного тушения люминесценции Ce^{3+} GAG определен как термически индуцированная ионизация ионов Ce^{3+}.

1. Introduction

$Gd_3(Al,Ga)_5O_{12}$ (GAGG) gadolinium aluminum-gallium garnets doped with Ce^{3+} ions are used as the effective phosphors for white light-emitting diodes (LEDs). Their development was stimulated by the well-known shortcomings of white LEDs based on $Y_3Al_5O_{12}:Ce^{3+}$ (YAG:Ce^{3+}); these are a low color rendering index ($R_a < 80$) and a high color temperature (>4000 K). This caused the attempts to improve the color characteristics of LEDs by substitution of Y^{3+} with other rare earth (R) ions including Gd^{3+} [1–3]. Rare earth aluminates $R_3Al_5O_{12}$ (R = Y, Eu–Lu) crystallize in the cubic structure with the *Ia3d* space group. In this structural type, all R atoms are dodecahedrally coordinated, whereas Al atoms occupy two crystallographically nonequivalent positions — namely, tetrahedral (Al_{tetr}) and octahedral (Al_{oct}) sites. The substitution of Gd^{3+} for Y^{3+} was shown to induce a larger crystal field splitting of the Ce^{3+} 5*d* configuration and to shift the Ce^{3+} emission band towards longer wavelengths [1, 4, 5].

Single crystals and ceramic materials of the general composition $Gd_3(Al,Ga)_5O_{12}:Ce^{3+}$ are of interest for the development of new scintillators for medical applications due their extremely high light output (up to 70000 ph/MeV), relatively fast scintillation response and high radiation stability [6, 7]. Some GAGGs double doped with Ce^{3+} and Cr^{3+} are also considered as persistent phosphors for luminous paints and as perspective luminescent materials with long afterglow for directed *in vivo* bioimaging [8, 9].

In contrast to GAGG, information on the luminescence properties of Ce^{3+}-doped gadolinium aluminum garnet $Gd_3Al_5O_{12}$ (GAG) is limited by few studies [4, 5, 10], probably due to a thermodynamic instability of this compound [11, 12]. The exact reason for thermodynamic instability of GAG is still unknown, but it is usually associated with a critically large ratio between the sizes of rare earth and aluminum polyhedra for this structural type [11, 12]. Meanwhile, GAG:Ce^{3+} is known to exhibit a broad-band emission with FWHM 133 nm (3730 cm^{-1}) and is a promising phosphor for medium power LEDs with a comfortable warm white light because of the longer wavelength position (585 nm) of its emission maximum [5] compared to those of Ce^{3+}-doped GAGG and YAG. Besides this, the development of magnetic-luminescent Ce^{3+}-doped GAG nanoparticles for simultaneous imaging and X-ray photodynamic therapy of cancer cells has been recently reported [13].

Despite the practical importance of Ce^{3+}-doped GAG phosphors, no detailed research has been performed on the influence of temperature on its luminescence properties. In this paper, we describe the results of the study of $Gd_{3(1-x)}Ce_{3x}Al_5O_{12}$ ($x = 0.01$) luminescence in the temperature range of 77–500 K. In particular, our attention was focused on the mechanism for temperature quenching of Ce^{3+} emission in GAG. A comparison with the results on other compounds of the garnet family is also carried out. It is expected that the results obtained will be significant not only for the interpretation of the influence of substitutional ions (N^{3-}, Mg^{2+}, Si^{4+}) on the luminescence properties of Ce^{3+}-doped GAG, but also for the development of new garnet-type phosphors for white LEDs.

2. Experimental

Two samples with compositions of $Gd_{3(1-x)}Ce_{3x}Al_5O_{12}$ ($x = 0.01$) (GAG:Ce^{3+}) and $(Gd_{0.50}Y_{0.50})_{3(1-x)}Ce_{3x}Al_5O_{12}$ ($x = 0.01$) (GYAG:Ce^{3+}) were obtained by the co-precipitation of REE and aluminum hydroxides with their further thermal decomposition [5]. The appropriate amounts of Gd_2O_3, Y_2O_3 (99.99 %, Sigma-Aldrich) and CeO_2 (99.99 %, Sigma-Aldrich) were dissolved in a dilute HNO_3 solution and mixed homogeneously with a water solution of aluminum nitrate $Al(NO_3)_3 \cdot 9H_2O$ (99 %). The hydrous mixed REE and aluminum hydroxides $M(OH)_3 \cdot nH_2O$ were precipitated from the hot solution (80°C) by the slow addition of a concentrated NH_4OH solution. The precipitates were filtered, washed with distilled water, dried and then heated at 1000°C for 3 h in air. After that the resulting mixtures were fired at a temperature of about 1300°C for 15 h in a reducing medium created by burning activated carbon. The samples were characterized by X-ray diffraction (XRD) using Cu–K_α radiation (Rigaku Ultima IV). The morphological investigations were carried out by scanning electron microscopy (SEM) on a TESCAN VEGA 3 electron microscope. The emission and excitation spectra in the UV-visible region were obtained using a Fluorolog FL-3 (Horiba Jobin Yvon) spectrofluorometer equipped with a xenon lamp. Note, that the GYAG:Ce^{3+} sample was used to control the synthesis procedure and as a reference sample for measuring the quantum efficiency of luminescence.

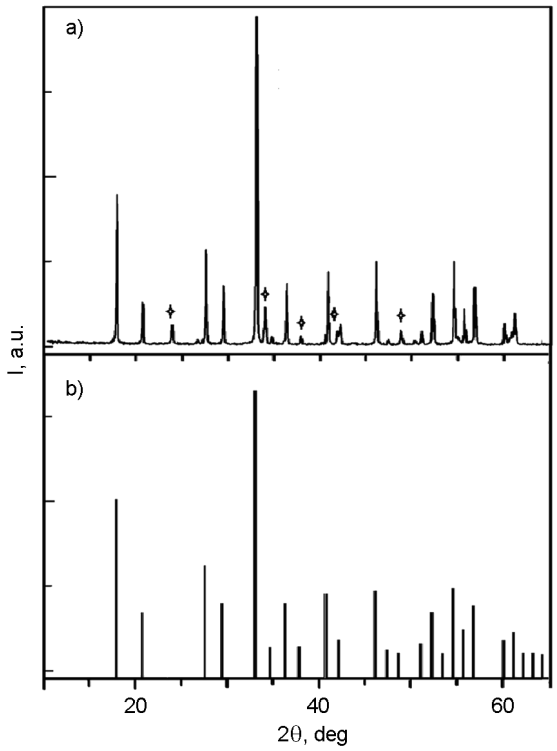

Fig. 1. Comparison of X-ray diffraction pattern (a) — of the GAG:Ce^{3+} with (b) — data from ICDD database (PDF #73-1371) for pure GAG. Peaks from the impurity phase ($GdAlO_3$) are denoted by the symbols (✧).

The excitation spectra at wavelengths shorter than 330 nm were recorded at 293 K using synchrotron radiation and the equipment of the SUPERLUMI experimental station at HASYLAB (Hamburg, Germany). The correction of these spectra for the wavelength dependent excitation intensity was performed with the use of sodium salicylate as a standard. The decay curves of the Ce^{3+} emission were recorded in the temperature range from 77 to 500 K using the time-correlated single-photon counting method upon excitation with either nanosecond LEDs with λ_{max} at 330 and 450 nm or a flash lamp with discharge in air.

3. Results and discussion

No impurity phases were detected from the XRD pattern of the GYAG:Ce^{3+} sample. In contrast, the XRD pattern of the GAG:Ce^{3+} revealed, in addition to $Gd_3Al_5O_{12}$, the presence of some amounts of the $GdAlO_3$ phase (see Fig. 1).

From the obtained peaks in the XRD pattern, a lattice constant of the GAG:Ce^{3+}

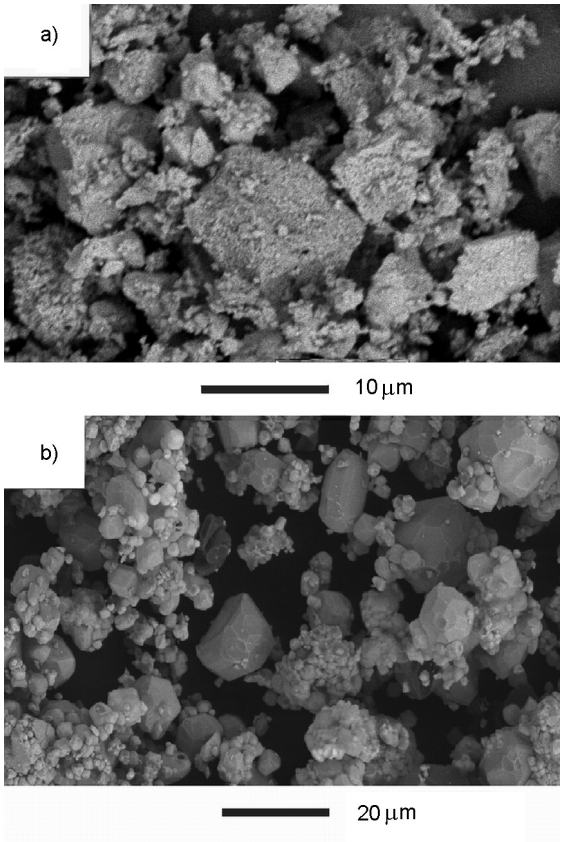

Fig. 2. SEM images of (a) — GAG:Ce^{3+} and (b) — GYAG:Ce^{3+}.

was calculated using the Bragg's law for cubic crystals:

$$\alpha = \frac{\lambda\sqrt{h^2 + k^2 + l^2}}{2\sin\theta}, \qquad (1)$$

where λ is the Cu–K_α X-ray wavelength; h, k, and l are Miller's indices; and θ is the diffraction angle.

The calculated lattice constant of 12.11 Å agrees well with the literature data for pure GAG [14]. The SEM images of the samples are compared in Fig. 2. As can be seen, the GYAG:Ce^{3+} sample is composed of crystallites with a size of 1–15 μm, which exhibit a relatively low degree of agglomeration. It should also be noted the presence of crystallites with smooth trapezium-shaped faces (Fig. 2b), which is quite typical for compounds and solid solutions of the garnet family. In contrast, the SEM image of the GAG:Ce^{3+} revealed the presence of agglomerated particles with sizes of 1–10 μm and with a poorly defined habitus. Thus, the particle morphology of the GAG:Ce^{3+} differs markedly from that of GYAG. This is most likely due to the thermodynamic instability of this compound.

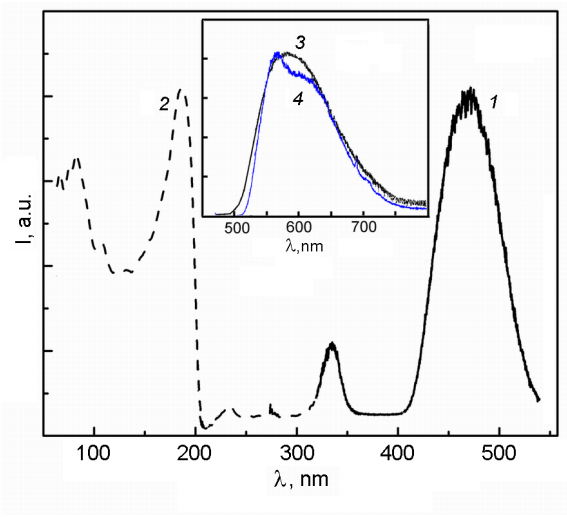

Fig. 3. Time-integrated excitation spectrum of Ce^{3+} emission in GAG (λ_{em} = 560 nm) recorded upon excitation with optical photons (*1*) and synchrotron radiation (*2*). The inset shows the emission spectra of the sample at (*3*) 293 K and (*4*) 77 K (λ_{exc} = 445 nm).

Since the luminescence properties of Ce^{3+} ions in the garnets are distinctly different from those of Ce^{3+} in $RAlO_3$ (R = Y, Gd), the presence of this impurity phase did not prevent the selective excitation and detection of the luminescence of Ce^{3+} ions in GAGs. It is known that the emission spectrum of the GAG doped with Ce^{3+} is due to transitions from the lowest Ce^{3+} $5d$ excited state to the $4f$ ground state levels $^2F_{5/2}$ and $^2F_{7/2}$ [4, 5]. The emission spectra of Ce^{3+} ions in GAG at 293 and 77 K are compared in Fig. 3. It is seen that at room temperature, the Ce^{3+} emission band of the GAG:Ce^{3+} extends from 470 to 800 nm and has a maximum at about 585 nm. Note, that the position of the emission maximum is somewhat different from the position (~ 600 nm) indicated by Ogieglo et al. for GAG prepared by the sol-gel method [4]. At 77 K, the emission band of the Ce^{3+}-doped GAG is narrowed and has a distinct maximum at 564 nm and a shoulder at about 620 nm.

The time-integrated emission spectrum at room temperature, recorded upon excitation of Ce^{3+} in the GAG by synchrotron radiation and optical photons, is shown in Fig. 3. The spectrum consists of relatively narrow bands around 275 nm and broad bands with maxima at about 230, 335 and 471 nm. In the excitation spectrum of YAG doped with Ce^{3+}, the narrow bands are absent and should be attributed to the $^8S_{7/2} \rightarrow {}^6I_J$ transitions of Gd^{3+} ions, while the broad

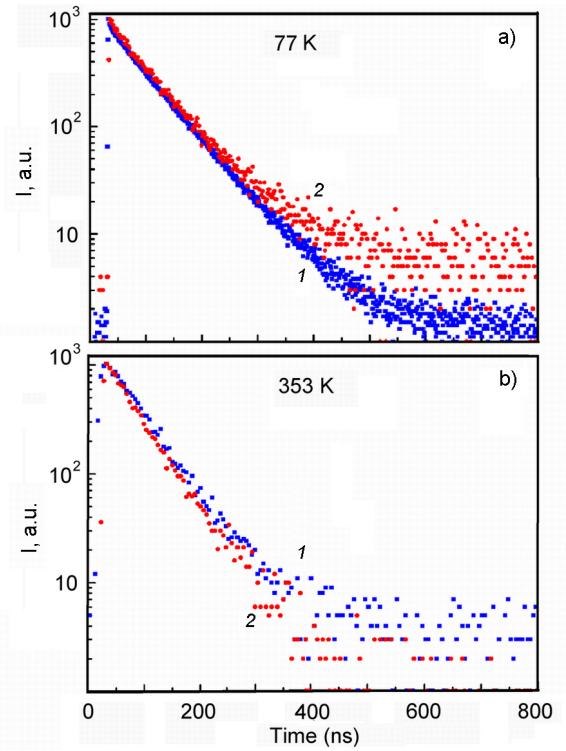

Fig. 4. Decay curves of Ce^{3+} emission (λ_{em} = 560 nm) for GAG:Ce^{3+} recorded at 77 K (a) and 353 K (b) upon excitation with λ_{exc} = 450 nm (*1*) and 340 nm (*2*).

ones with maxima at 471 and 335 nm are due to the $4f \rightarrow 5d$ transitions with two components ($5d_{1,2}$) of the Ce^{3+} $5d$ configuration [4, 5].

The lower-intensity band at ~ 230 nm exhibits a distinct asymmetric shape and can be approximated by two Gaussians with maxima at 5.34 eV (232 nm) and 5.58 eV (222 nm), which are considered as a result of the $4f \rightarrow 5d_{3,4}$ transitions. As with many other garnets, the $4f \rightarrow 5d_5$ transition of Ce^{3+} in GAG is expected to overlap with the host absorption band starting at 206 nm and peaking at about 187 nm (6.63 eV). Note that the similar peaks were observed earlier in the excitation spectra for the Ce^{3+} emission in various garnets, including YAG, $Lu_3Al_5O_{12}$ (LuAG), and were attributed either to the absorption of the host exciton or to the formation of a (Ce^{3+})-bound impurity exciton [4, 9, 15–17].

The quantum efficiency (QE) of luminescence of the GAG:Ce^{3+} sample was determined as described in [1], using a commercial YAG:Ce^{3+} phosphor for LEDs with *QE* = 0.90 as a standard. For the excitation at 455 nm, the found value of 0.58±0.04 is larger

than that (QE = 0.32) of the Ce^{3+} emission in the nanosized GAG obtained by the sol-gel method [13], but smaller than those (QE = 0.80–0.85) reported in literature for Ce^{3+} ions in ceramic phosphors of the $Gd_{3(1-x)}Y_{3x}Al_5O_{12}$ (x = 0.25; 0.50) composition [9].

The decay curves of the Ce^{3+} emission in the GAG at 77 K and 353 K upon excitation of $4f \rightarrow 5d_{1,2}$ bands are compared in Fig. 4. It is seen that at 77 K the decay curves are similar and can be characterized by a time constant of $\tau = 68.4 \pm 0.5$ ns. For λ_{exc} = 340 nm, the decay curve has a distinctly higher background level. Although the Ce^{3+} $5d_2$ level is expected to be within the conduction band (CB) of the GAG, the high background level is attributed to the low signal-to-noise ratio caused by the low absorption strength for the $4f \rightarrow 5d_2$ transition at 77 K [5]. This suggestion is supported by the fact that at higher temperatures (270–500 K) the decay curves are also similar and no high background level for the decay curves recorded upon excitation with λ_{exc} = 340 nm is observed. As an example, a comparison of the decay curves at 353 K is presented in Fig. 4b. It is seen that the decays are one-exponential with a time constant of ~ 53.0 ns.

Figure 5 shows the temperature dependences of the luminescence decay kinetics and decay time (τ) for Ce^{3+} ions in GAG upon excitation of the Ce^{3+} $5d_2$ state (λ_{exc} = 340 nm) in the range of 270–500 K. It can be seen that at 310 K the emission decay time begins to decrease, and at 395 K it is ~ 50 % of its value at room temperature. This behavior agrees with the experimental results for Ce^{3+}-doped $Gd_3Al_{5-x}Ga_xO_{12}$ (x = 1–4) [4]. The activation energy of the process responsible for the temperature quenching of Ce^{3+} emission in GAG was calculated from the temperature dependence of τ using the Mott formula:

$$\tau(T) = \frac{\tau_0}{1 + Ce^{-E_a/kT}}, \qquad (2)$$

where $\tau(T)$ is the decay time of emission at temperature T (K), τ_0 is the luminescence decay time at low temperatures, C is a constant, E_a is the activation energy for the quenching process (eV), and k is the Boltzmann constant ($8.6173 \cdot 10^{-5}$ eV/K).

The activation energy for temperature quenching of Ce^{3+} luminescence in GAG was determined as 0.51±0.04 eV by fitting the

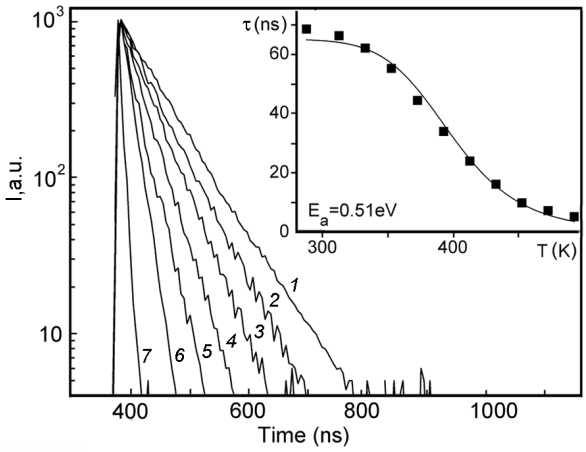

Fig. 5. Temperature dependences of the luminescence decay kinetics of Ce^{3+} ions in GAG recorded upon excitation with λ_{exc} = 340 nm: *1* — 288; *2* — 353; *3* — 373; *4* — 393; *5* — 413; *6* — 433; *7* — 473 K. The inset shows the temperature dependence of the luminescence decay time.

experimental data to Eq. (2). A similar result was obtained upon excitation of the Ce^{3+} $5d_1$ state (λ_{exc} = 450 nm).

The mechanism for temperature quenching of Ce^{3+} emission in various compounds with a garnet structure is still under discussion [16, 18–21]. In general, two mechanisms can be responsible for the temperature quenching of the $5d \rightarrow 4f$ luminescence of Ce^{3+} in inorganic compounds: (i) quenching by thermally activated cross-over from the $5d_1$ excited state to the $4f$ ground state and (ii) thermally activated ionization of Ce^{3+} ions for the $5d_1$ state.

Recently, strong arguments have been summarized in support of the opinion that the temperature quenching of Ce^{3+} emission in the most practically important series of compounds with a garnet structure is caused by thermally induced ionization of Ce^{3+} ions [16]. For example, by an analysis of thermoluminescence (TL) excitation spectra at 300–700 K for YAG:Ce^{3+}, it was shown that there is a good agreement between the temperature quenching of the Ce^{3+} emission in YAG and the appearance and rise of TL signal in the range of 500–700 K. Also, based on the photoconductivity measurements of a series of Ce^{3+}-doped $Y_3(Al,Ga)_5O_{12}$ and $Gd_3(Al,Ga)_5O_{12}$ garnets, the quenching mechanism was determined as a thermal ionization process [16] and references therein). In contrast, the authors [20, 21] have recently analyzed the temperature dependences of the instantaneous and

delayed recombination decays in Ce^{3+}-doped $(Gd,Y)_3Al_5O_{12}$ and $Gd_3(Al,Ga)_5O_{12}$ single crystals and came to the conclusion that the quenching of luminescence is mainly caused by thermally induced cross-over from the excited $5d_1$ state to the ground $4f$ state and can be slightly assisted by the thermally activated ionization process in garnets with a high Ga content. It should be noted that both of these mechanisms were also used to interpret the decrease in the integrated emission intensity and luminescence decay time of Ce^{3+} with increasing temperature from 300 to 700 K in oxynitride garnet phosphors $(Y,Cd)_3(Al,Si)_5(O,N)_{12}$ [22, 23].

Ce^{3+}-doped $Ca_3Sc_2Si_3O_{12}$ and LuAG are known to exhibit the highest thermal stability of emission among the known Ce^{3+}-doped phosphors of the garnet family [16, 24]. In particular, the decay time of Ce^{3+} emission in $Ca_3Sc_2Si_3O_{12}$ was found to be nearly constant up to 800 K [24, 25]. On the contrary, it can be seen from Fig. 5 that the thermal quenching of Ce^{3+} emission in GAG begins at 310 K, and the quenching temperature ($T_{50\%}$) defined as the temperature at which the emission decay time equals half of those at low temperature, is found to be ~ 395 K, which is 300–400 K lower than for YAG, LuAG doped with Ce^{3+} [16].

If the quenching process in GAG involves the thermal ionization of Ce^{3+} ions, the quenching temperature ($T_{50\%}$) should be determined by the energy gap (ΔE) between the $5d_1$ state and the bottom of the conduction band (CB). For comparison with the experimental data and calculated values of ΔE for Ce^{3+}-doped $Gd_3Al_{5-x}Ga_xO_{12}$ (x = 1–4) [9], we plotted the so-called vacuum referred binding energy (*VRBE*) diagram for GAG (see Fig. 6) according the procedure proposed earlier by Dorenbos [15] and used in [9]. The top of the valence band (E_V) for GAG was obtained by subtracting the charge transfer energy of Eu^{3+} in the GAG (E^{CT} = 5.37 eV [26]) from the $4f$ ground state energy of Eu^{3+} (–4.06 eV for all the garnets [15]). The found value E_V of –9.43 eV for the GAG is close to that found in [9] for $Gd_3Al_4GaO_{12}$ (–9.42 eV) and slightly less than for $Gd_3Al_{5-x}Ga_xO_{12}$ with x = 2–4.

The band gap energy (E_g) of GAG was estimated from the position of the exciton peak at 6.625 eV (~ 187 nm) (see Fig. 3) by adding the exciton binding energy [27]: $0.008 \cdot (E^{ex})^2 = 0.367$ eV. Since the luminescence excitation spectra (Fig. 3) were recorded at 293 K, the host exciton creation

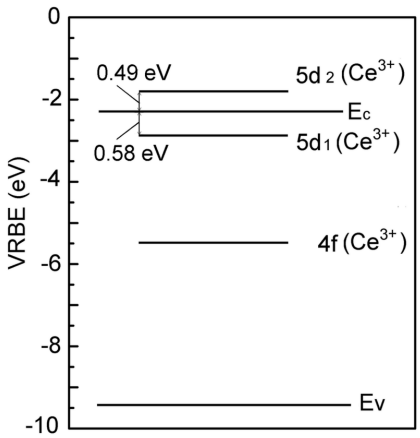

Fig. 6. *VRBE* diagram of GAG with Ce^{3+} $5d$ levels.

energy (E^{ex}) was corrected by adding 0.15 eV before multiplying. This gives a value of E_g = 7.14 eV. To estimate the energy of the bottom of the conduction band (E_C) for GAG, the band gap energy (7.14 eV) was then added to E_V. The found value E_C of –2.29 eV appeared to be somewhat higher than for $Gd_3Al_{5-x}Ga_xO_{12}$ (x = 1–4). In the approach used, the $4f$ ground state energy for Ce^{3+} is assumed to be constant, E_{4f} (Ce^{3+}) = –5.50 eV, within the Gd garnet series [15], so that the energies of the Ce^{3+} $5d_1$ and $5d_2$ states can be found by adding the $4f \rightarrow 5d_{1,2}$ transition energies to E_{4f} (Ce^{3+}). From comparison between the value E_C (–2.29 eV) and the found energies of the Ce^{3+} $5d_1$ and $5d_2$ states it follows that the energy gap (ΔE) between the $5d_1$ level and the bottom of the CB is 0.58 eV for GAG, and the $5d_2$ level is located above the CB bottom by ~ 0.49 eV.

In Table, the thermal quenching activation energies E_a of Ce^{3+} emission and the calculated energy differences (ΔE) between the $5d_1$ level of Ce^{3+} and the bottom of the conduction band for $Gd_3(Al,Ga)_5O_{12}$ garnets are presented and compared. It can be seen that there are distinct differences between the presented experimental results. For example, the reported activation energy for Ce^{3+} emission quenching in $Gd_3Al_2Ga_3O_{12}$ varies from 0.20 eV [29] to 0.33 eV [30]. It is possible that the observed differences are, at least in part, caused by the presence of defects in the immediate environment of Ce^{3+} ions; thermally activated transfer of electrons from Ce^{3+} can occur to these defects. The nature and concentration of such defects are evidently dependent on the synthesis conditions. In particular, a possible

Table. Thermal quenching activation energies E_a of Ce^{3+} emission and calculated energy differences (ΔE) between the $5d_1$ level of Ce^{3+} and the bottom of the conduction band for some garnets

Garnet	E_a, eV			ΔE, eV
$Gd_3Al_5O_{12}$	0.51[a]	–	–	0.58
$Gd_3Al_4GaO_{12}$	0.41[a] [4]	0.38[b] [28]	0.40[c] [30]	0.41 [9]
$Gd_3Al_3Ga_2O_{12}$	0.46[a] [4]	0.39[b] [28]	0.42[c] [30]	0.38 [9]
$Gd_3Al_2Ga_3O_{12}$	0.26[a] [4]	0.30[b] [28]; 0.20[b] [29]	0.33[c] [30]	0.31 [9]
$Gd_3AlGa_4O_{12}$	0.07[a] [4]	–	0.34[c] [30]	0.25 [9]

[a] powder phosphor; [b] opaque ceramic; [c] single crystal.

role of Ga^{3+} ions and oxygen vacancies in the processes of defect formation in $Gd_3(Al,Ga)_5O_{12}$ garnets was discussed earlier [30]. From the *VRBE* diagrams it follows that if the quenching process involves the thermal ionization of Ce^{3+} ions, the activation energy for Ce^{3+} emission quenching in $Gd_3Al_{5-x}Ga_xO_{12}$ should steadily decrease with increasing Ga content (x) from 0.58 eV for GAG ($x = 0$) to ~ 0.25 eV for $Gd_3AlGa_4O_{12}$ ($x = 4$). From Table one can conclude that the expected tendency coincides in general with the experimental data.

It should be noted that, at high temperatures, for $Gd_3(Al,Ga)_5O_{12}$ garnets with a high Ga content, the decay of Ce^{3+} luminescence has a complex, nonexponential character. It is believed that the initial fast decay component is associated with the ionization of the Ce^{3+} (i.e. with the temperature quenching of luminescence) and the second, slow component, is due to the thermostimulated release of electrons from the traps with their subsequent recombination on Ce^{4+} centers [29, 31].

Although we did not observed any thermostimulated luminescence process that prolongs the decay of Ce^{3+} emission in GAG at high temperatures (310–500 K), we attribute the quenching of the Ce^{3+} luminescence in this garnet to the thermal ionization of the impurity ions. This interpretation is based on the following facts. In Ce^{3+}-doped $Gd_3(Al,Ga)_5O_{12}$ garnets, the energy of the $5d_1 \rightarrow 4f$ ($^2F_{5/2}$) transition maximum increases steadily with an increase in the Ga content from 2.198 eV (564 nm) for GAG (see Fig. 3) to 2.36 eV (~ 525 nm) for $Gd_3AlGa_4O_{12}$ [30]. Therefore, it is expected that the activation energy of the cross-over from the excited $5d_1$ state to the ground $4f$ state increases, but the quenching temperature $T_{50\%}$ decreases from ~ 395 K for GAG, as found in this study, to 175 K for $Gd_3AlGa_4O_{12}$ [4].

The *VRBE* diagrams of $Gd_3(Al,Ga)_5O_{12}$ indicate that the energy gap between the excited $5d_1$ state and the bottom of CB decreases gradually with increasing Ga content, which means a decrease in the activation energy of the quenching process caused by thermal ionization of Ce^{3+} ions. Taking into account possible errors in both the experimental results and in the energy level diagram, it follows from Table that this trend is generally reproduced in the experiments.

5. Conclusions

Gadolinium aluminum garnet (GAG) doped with Ce^{3+} ions was prepared by the co-precipitation method. The luminescent properties of Ce^{3+} ions in $Gd_{3(1-x)}Ce_{3x}Al_5O_{12}$ ($x = 0.01$) were studied in the temperature range of 77–500 K. At 293 K the Ce^{3+}-doped GAG exhibits a broad-band emission with a maximum at 585 nm and a decay time of 68.4 ns. It was shown that the temperature quenching of Ce^{3+} emission in GAG begins at 310 K and the quenching temperature ($T_{50\%}$) is 395 K. From the temperature dependence of the luminescence decay time upon excitation into both Ce^{3+} $4f \rightarrow 5d_{1,2}$ bands, it was found that the activation energy for the Ce^{3+} emission quenching in GAG was 0.51 eV.

Based on the results of luminescence measurements and comparison with literature data for $Gd_3(Al,Ga)_5O_{12}$ garnets the quenching mechanism in Ce^{3+}-doped GAG was determined as the thermally induced ionization of Ce^{3+} ions. In particular, in Ce^{3+}-doped $Gd_3(Al,Ga)_5O_{12}$, the energy of the $5d_1 \rightarrow 4f$ ($^2F_{5/2}$) transition maximum increases steadily with an increase in the Ga content from 2.198 eV (564 nm) for

GAG to 2.36 eV (~ 525 nm) for $Gd_3AlGa_4O_{12}$, but the quenching temperature $T_{50\%}$ decreases from ~ 395 K for GAG to 175 K for $Gd_3AlGa_4O_{12}$, supporting the conclusion that the quenching process in GAG involves the thermal ionization of Ce^{3+} ions.

At 293 K, the quantum efficiency (QE) of the Ce^{3+} emission in the GAG:Ce^{3+} is 0.58 and less than those (QE = 0.80–0.85) reported in the literature for Ce^{3+}-doped $Gd_{3(1-x)}Y_{3x}Al_5O_{12}$ (x = 0.25; 0.50). It can be expected that improved methods of preparing powders can contribute to some improvement in the luminescence characteristics of GAG:Ce^{3+} phosphors for white LEDs.

References

1. V.Bachmann, Thesis, Utrecht, Universiteit Utrecht (2007).
2. C.C.Chiang, M.S.Tsai, M.H.Hon, *J. Electrochem. Soc.*, **154**, J326 (2007).
3. J.Y.Park, H.C.Jung, G.S.R.Raju et al., *Opt. Mater.*, **32**, 293 (2009).
4. J.M.Ogieglo, A.Katelnikovas, A.Zych et al., *J. Phys. Chem. A*, **117**, 2479 (2013).
5. V.P.Dotsenko, I.V.Berezovskaya, A.S.Voloshinovskii et al., *Mater. Res. Bull.*, **64**, 151 (2015).
6. K.Kamada, T.Endo, K.Tsutsumi et al., *Cryst. Growth Des.*, **11**, 4484 (2011).
7. T.Yanagida, K.Kamada, Y.Fujimoto et al., *Opt. Mater.*, **35**, 2480 (2013).
8. K.Asami, J.Ueda, S.Tanabe et al., *Opt. Mater.*, **62**, 171 (2016).
9. K.Asami, J.Ueda, M.Kitaura et al., *J. Luminescence*, **198**, 418 (2018).
10. E.J.Popovici, M.Morar, E.Bica et al., *J. Optoelectron. Adv. Mater.*, **13**, 617 (2011).
11. Y.Kanke, A.Navrotsky, *J. Solid State Chem.*, 141, 424 (1998).
12. J.Li, J.G.Li, Z.Zhang et al., *J. Am. Ceram. Soc.*, **95**, 931 (2012).
13. A.Jain, R.Koyani, C.Munoz et al., *J. Colloid Interf. Sci.*, **526**, 220 (2018).
14. A.C.Sackville Hamilton, G.I.Lampronti et al., *J. Phys. Condens. Matter.*, **26**, 116001 (2014).
15. P.Dorenbos, *J. Luminescence*, **134**, 310 (2013).
16. J.Ueda, S.Tanabe, *Opt. Mater.: X*, **1**, 100018 (2019).
17. I.V.Berezovskaya, V.P.Dotsenko, A.S.Voloshinovskii et al., *Chem. Phys. Lett.*, **585**, 11 (2013).
18. Y.Ch.Lin, M.Bettinelli, M.Karlsson, *Chem. Mater.*, **31**, 3851 (2019).
19. S.Arjoca, D.Inomata, Y.Matsushita et al., *Cryst. Eng. Comm.*, **18**, 4799 (2016).
20. K.Bartosiewicz, V.Babin, K.Kamada et al., *Opt. Mater.*, **63**, 134 (2017).
21. K.Bartosiewicz, V.Babin, K.Kamada et al., *J. Luminescence*, **216**, 116724 (2019).
22. L.Ning, X.Ji, Y.Dong et al., *J. Mater. Chem. C*, **4**, 5214 (2016).
23. K.Asami, J.Ueda, M.Shiraiwa et al., *Opt. Mater.*, **87**, 117 (2019).
24. I.V.Berezovskaya, Z.A.Khapko, A.S.Voloshinovskii et al., *J. Luminescence*, **195**, 24 (2018).
25. S.K.Sharma, Y.Ch.Lin, I.Carrasco et al., *J. Mater. Chem. C*, 6, 8923 (2018).
26. I.Carvalho, A.J.S.Silva, P.A.M.Nacimento et al., *Opt. Mater.*, **98**, 109449 (2019).
27. P.Dorenbos, *Opt. Mater.*, **69**, 8 (2017).
28. I.Venetsev, V.Khanin, P.Rodnyi et al., *IEEE Trans. Nucl. Sci.*, **65**, 2090 (2018).
29. T.Lesniewski, S.Mahlik, K.Asami et al., *Phys. Chem. Chem. Phys.*, **20**, 18380 (2018).
30. L.Grigorjeva, K.Kamada, M.Nikl et al., *Opt. Mater.*, **75**, 331 (2018).
31. Y.Wu, M.Nikl, V.Jary et al., *Chem. Phys. Lett.*, **574**, 56 (2013).